AIP | Physics of Plasmas

K-shell emission trends from 60 to 130cm/s stainless steel implosions

D. J. Ampleford, C. A. Jennings, B. Jones, S. B. Hansen, M. E. Cuneo, C. A. Coverdale, M. C. Jones, T. M. Flanagan, M. Savage, W. A. Stygar, M. R. Lopez, J. P. Apruzese, J. W. Thornhill, J. L. Giuliani, and Y. Maron

Citation: Physics of Plasmas (1994-present) **20**, 103116 (2013); doi: 10.1063/1.4823711
View online: http://dx.doi.org/10.1063/1.4823711
View Table of Contents: http://scitation.aip.org/content/aip/journal/pop/20/10?ver=pdfcov
Published by the AIP Publishing

K-shell emission trends from 60 to 130 cm/μs stainless steel implosions

D. J. Ampleford,[1,a)] C. A. Jennings,[1] B. Jones,[1] S. B. Hansen,[1] M. E. Cuneo,[1]
C. A. Coverdale,[1] M. C. Jones,[1] T. M. Flanagan,[1] M. Savage,[1] W. A. Stygar,[1]
M. R. Lopez,[1] J. P. Apruzese,[2,b)] J. W. Thornhill,[2] J. L. Giuliani,[2] and Y. Maron[3]
[1]*Sandia National Laboratories, Albuquerque, New Mexico 87106, USA*
[2]*Naval Research Laboratory, Washington, DC 20375, USA*
[3]*Weizmann Institute of Science, Rehovot 76100, Israel*

(Received 29 May 2013; accepted 9 September 2013; published online 21 October 2013)

Recent experiments at the 20 MA Z Accelerator have demonstrated, for the first time, implosion velocities up to 110–130 cm/μs in imploding stainless steel wire arrays. These velocities, the largest inferred in a magnetically driven implosion, lead to ion densities of $2 \times 10^{20}\,\mathrm{cm}^{-3}$ with electron temperatures of ~5 keV. These plasma conditions have resulted in significant increases in the K-shell radiated output of 5–10 keV photons, radiating powers of >30 TW and yields >80 kJ, making it the brightest laboratory x-ray source in this spectral region. These values represent a doubling of the peak power and a 30% increase in the yield relative to previous studies. The experiments also included wire arrays with slower implosions, which were observed to have lower temperatures and reduced K-shell output. These colder pinches, however, radiated 260 TW in the soft x-ray region, making them one of the brightest soft x-ray sources available. © *2013 AIP Publishing LLC*. [http://dx.doi.org/10.1063/1.4823711]

I. INTRODUCTION

High velocity, magnetically driven implosions of stainless steel wire arrays provide extreme plasma conditions and are the most powerful and energetic source of 5–10 keV photons currently available.[1] As an x-ray source, these wire arrays have the potential to drive physics experiments such as photo-ionization experiments in which inner-shell absorption is desired or to act as an intense source for scattering studies, such as x-ray Thomson scattering. Multi-mega-Ampere currents delivered by low impedance multi-module pulsed power generators efficiently implode nested wire array z-pinches via the J × B Lorenz force.[2] Significant investigations[1,3–5] have previously been carried out aimed at understanding mechanisms for K-shell emission from nested wire arrays and the suggested tradeoffs necessary to optimize the energy radiated from K-shell transitions, which are >5 keV (the 'K-shell yield'). However, for the previous work, the implosion velocity was not measured directly, but rather inferred through implosion dynamics models.

In this paper, we show for the first time how plasma conditions and radiative properties achieved at peak compression for these systems vary with experimentally inferred implosion velocities. Velocities of stainless steel wire array implosions on the refurbished Z generator are determined by the time delay between the interaction x-ray pulse (radiated as the outer wire array reaches the inner wire array[6,7]) and the final stagnation of the pinch, as well as by an in-depth understanding of the wire array implosion dynamics.[8–10] Comparison to implosion velocities determined by 2-dimensional and 3-dimensional Magneto-Hydrodynamic (MHD) simulations[9] indicates that this is a reliable measure of implosion velocity. Implosion velocities up to 130 cm/μs are inferred from the experiments, which are the largest reported for a magnetically driven implosion. These high implosion velocities thermalize at stagnation and enable the pinch to reach high temperatures and radiate efficiently in the 5–10 keV spectral range. To understand the impact of the implosion velocity on the plasma conditions and radiated output, we use time-integrated, spatially-averaged spectroscopy to determine how the plasma conditions in the stagnated plasma vary for different implosion velocities and how this impacts the radiation emitted. Additionally, the experiments described here utilized the refurbished Z generator, now coupling 20 MA to this type of experiment, thereby broadening the plasma conditions that can be achieved, and enabling higher K-shell yields.

The remainder of this paper is arranged as follows. In Sec. II, we discuss the plasma conditions necessary for efficient K-shell emission and how atomic physics can be used to establish the plasma conditions present. In Sec. III, we discuss a new technique for determining the implosion velocity of an imploding nested wire array. This technique is utilized in Sec. IV to investigate how stagnation temperature and the emitted K-shell power and yield vary with implosion velocity. We conclude with a summary in Sec. V.

II. REQUIREMENTS FOR STAINLESS STEEL K-SHELL EMISSION

Efficient K-shell emission from a stainless steel plasma requires a high plasma temperature and density.[11] Figure 1(a) shows the results of varying electron temperatures and ion number densities from a static collisional radiative equilibrium calculation (including opacity) for a uniform, static Fe plasma column of 0.9 mm diameter (the typical column diameter for these experiments, as determined by the full width at half maximum of pinhole-imaged >5 keV self-emission). Contours of constant K-shell power and the Fe

a)Email: damplef@sandia.gov
b)Consultant to NRL through Engility Corp., Chantilly, Virginia 20151, USA.

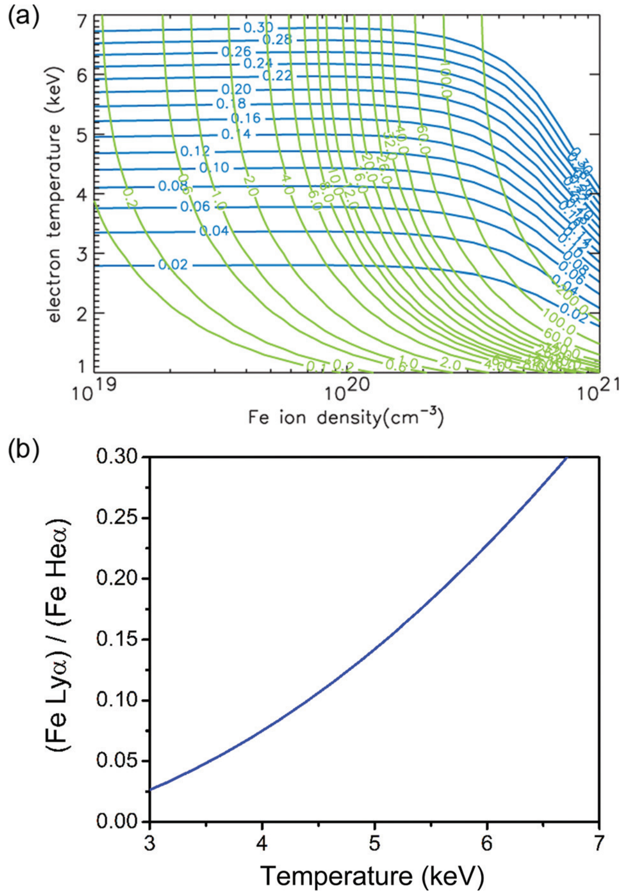

FIG. 1. (a) Variation of Fe Ly-α to Fe He-α ratio (blue) and K-shell power (green) in temperature-density space. Note that the density values shown are densities of Fe ions—the ion density of stainless steel including all species is 40% higher. (b) Variation of the line ratio with temperature for Fe ion densities $<3 \times 10^{20}\,\mathrm{cm}^{-3}$, where the ratio is independent of density.

Ly-α to Fe He-α line ratio are shown in the plot. The intensity of these diagnostically relevant lines is indicative of the relative population of different ionization states and, hence, are a strong diagnostic of the plasma temperatures necessary to reach this ionization state.[11] These contours indicate that, within this temperature and density regime, the K-shell power (green) increases with both increasing temperature and density. Comparing measured line ratios from time-integrated spectroscopy with the contours in Figure 1(a) can provide insight into the plasma conditions present in an experiment. The contours in Figure 1(a) show that the Fe Ly-α to Fe He-α line ratio is purely a function of temperature at densities $\leq 3 \times 10^{20}\,\mathrm{cm}^{-3}$; this relationship is shown in Figure 1(b). It is noted that, in this regime, while the photon escape probability is low (a few percent[12]), the majority of the photons are not absorbed and, instead, are scattered out of the pinch. Hence, in this case, the temperatures measured by this technique are reasonably characteristic of the entire K-shell emitting region.

Because these pinches consist of time-varying, non-uniform plasmas, the measured spectra interpreted in this way represent an average of the spectra over significant gradients in time and space. Previous work has indicated that the use of time-integrated spectra leads to an estimate of the temperature that is lower than the temperature achieved at peak compression.[13] Here, we use time-integrated spectroscopy as this enables a direct comparison between experiments. The use of time-resolved data would be sensitive to the timing of the spectra with respect to the implosion, so it would not capture the global comparison between experiments. In a future paper we will explore some of the details gleaned from time resolved spectroscopy for one of the experiments discussed here.

In a wire array z-pinch the rapid conversion of kinetic energy from a high velocity implosion is used to reach the conditions required for efficient K-shell emission. The minimum amount of $\mathbf{J} \times \mathbf{B}$ energy per ion required to ionize and heat the electrons from a given element (atomic number Z) into the K-shell is E_{min}; for elements of $Z \leq 36$, $E_{min} \sim 0.1012\, Z^{3.662}$ eV/ion.[14] The dimensionless parameter $\eta = K_i/E_{min}$ provides a simple comparison between the kinetic energy per ion (K_i) and E_{min}. Significantly more K_i than E_{min} must be transferred to the plasma to ensure that there is additional energy available to be radiated as K-shell emission and to overcome radiative losses from lower ionization stages encountered as the plasma ionizes into the K-shell. Previous work and experimental results indicate that values of $\eta \geq 2$ are a necessary requirement for radiating efficiently in the K-shell,[14] implying that to reach $T_e \sim 5$ keV for Fe ($Z = 26$, $A = 55.8$ amu) requires implosion velocities

$$v \sim \sqrt{\frac{2\eta E_{\min}}{m}} \sim \sqrt{\frac{2.024\,\eta\, Z^{3.662}}{A}} \sim 105\,\mathrm{cm}/\mu\mathrm{s}.$$

III. DETERMINATION OF IMPLOSION VELOCITY

The velocity of an imploding z-pinch plasma is a function of the initial load diameter and mass, and varies in space and time. Various models have been developed to understand the dynamics of K-shell producing pinches. In previous experiments, it has been assumed that the implosion reaches the peak velocity estimated by a 0-dimensional implosion model. Such models are highly sensitive to the choice of a final stagnation radius (or alternatively the convergence ratio). Recent work by Jones *et al.*[15] has begun to explore the use of Doppler splitting of the radiated lines to establish the implosion velocities. Such an approach provides an accurate measurement of the velocity of radiating ions; however, the plasma must have thermalized a fraction of the kinetic energy to generate the electron temperatures required for emission, so the plasma observed in this manner will have decelerated. Additionally, Doppler measurements sample the plasma that has been heated rather than providing a measure of the bulk plasma velocity. This is consistent with comparisons to simulations in Ref. 15, which indicated that the simulated Doppler velocities were lower than the calculated center-of-mass implosion velocities. Additionally, as observed in Ref. 15, Doppler velocity measurements are time varying, so for shot-to-shot comparisons a full time history of velocity must be established for each shot before comparisons can be made. To complement Doppler measurements, a new methodology has been developed to determine the characteristic implosion velocity.

In a nested wire array implosion, signatures are observed in the emitted radiation pulse when the implosion is at the

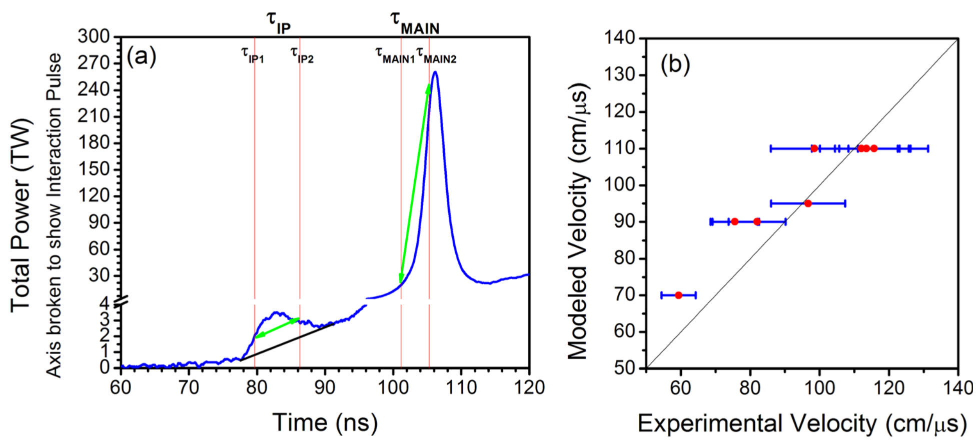

FIG. 2. (a) Total radiation pulses for an experiment with a 65 mm, 2.5 mg nested array. A split y-axis scale is used to show the interaction pulse and main pulse, which are identified by vertical lines. (b) Average velocities inferred from the relative timing of the interaction and main radiation pulses for a number of experiments at different masses and all three diameters, compared to center of mass implosions velocity estimates from simulations.

inner array location (the interaction pulse[6,7]) and when the implosion reaches the axis of symmetry (the rise of the main x-ray pulse[8]). These x-ray signatures are observable in the time-resolved pinch powers and x-ray yields that are measured with filtered photo conducting diodes (PCDs[16]), the silicon diode-based total energy and power diagnostic (TEP[17]), and thin-film bolometers (filtered Au bolometers and unfiltered Ni bolometers[18]). These signatures are evident in Figure 2, which shows the total emitted x-ray pulse for a 65-mm-diameter, 2.5-mg wire array, and are labeled IP and MAIN, respectively. Here, we use the relative delay between these two signatures along with the known geometric location of each to determine an average implosion velocity.

The interaction pulse, which is radiated as the outer array reaches the inner array (see Refs. 6 and 7 for a full discussion), is radiated at approximately the location of the inner array wires which is initially located at half the diameter of the outer array (ϕ_{array}). This interaction x-ray pulse has previously been used to determine different implosion modes within wire arrays.[19] Typically, this pulse is approximately Gaussian. For the measurements here, we take the time that this interaction pulse peaks (τ_{IP}) as representative when the bulk of the material is passing this location. Previous work[7] has established, using self-emission imaging, that this pulse is radiated when the implosion is approximately within the inner array inter-wire-gap ($\sim$0.5 mm in this case) after the implosion has passed the inner array (i.e., at smaller diameter).

The rise of the main x-ray pulse is associated with the arrival of material at the axis.[8] Here, we take the 50% point on the rise (τ_{Main}) as representative of the bulk of material arriving at the axis. Self-emission x-ray imaging of photons $>$5 keV in the present experiments indicates that this emission is from within 0.5 mm of the array axis.

Given the known initial outer array diameter ϕ_{array} and the use of an inner array that is half this diameter, the relative timing of features on the radiation pulse can be used to provide the velocity. The time between these two pulses $\Delta\tau$ and the distance travelled between them, $\Delta \mathrm{r} = \frac{\phi_{array}}{4} - 1\,\mathrm{mm}$, provide an average velocity between these two points in the implosion.

Combining these features, we find the implosion velocity to be

$$v_{imp} = \frac{\Delta r}{\Delta \tau} = \frac{\left(\frac{\phi_{array}}{4} - 1\mathrm{mm}\right)}{(\tau_{Main} - \tau_{IP})}.$$

Using this method, uncertainty in the exact location of the emitting regions in different experiments leads to a $\sim$5% uncertainty in the implosion velocity.

It is expected that there will be some range of velocities present in the imploding plasma, with likely variations between the leading and trailing edges of the implosion. To provide an estimate of this range, we expand the above measurement by providing estimates of the leading edge velocity (with a delay time given by the first 50% point on the interaction pulse and the 10% point on the rise of the main x-ray pulse) and the trailing edge velocity (with a delay time given by the second 50% point on the interaction pulse and the 90% point on the main x-ray pulse). The transit time for the front edge is denoted by the time difference between the start of the interaction pulse and the start of the rise of the main x-ray pulse. The back-edge transit time is defined as the time difference between the end of the interaction pulse and the end of the rise of the main x-ray pulse. These times are labeled τ_{IP1}, τ_{IP2}, τ_{MAIN1}, and τ_{MAIN2} in Figure 2(a). In the plots in Figure 2(b) and later, error bars in velocity reflect the range of velocities (i.e., the front edge velocity and the back edge velocities) along with the uncertainties in the location from which the emission originates.

These experimentally measured implosion velocities can be compared to those provided by 2-dimensional Gorgon MHD simulations[9,20] (see Figure 2(b)). These simulations have previously been validated against several other direct measurements.[9,15] As seen in Figure 2(b), the simulated and experimental velocities show reasonable agreement, providing confidence in this method. Moreover, analysis of a simulated total radiation pulse, shown in Figure 3(a), can be carried out by the same technique as used on the experimental data and provides a velocity estimate consistent with the center-of-mass velocity from the same simulation (as shown in Figure 3(b)). Finally, the simulations indicate that the velocity has dropped somewhat at the time of main pulse emission due to thermalization of kinetic energy. This deceleration has negligible effect on the time delay between the interaction pulse and the main pulse;

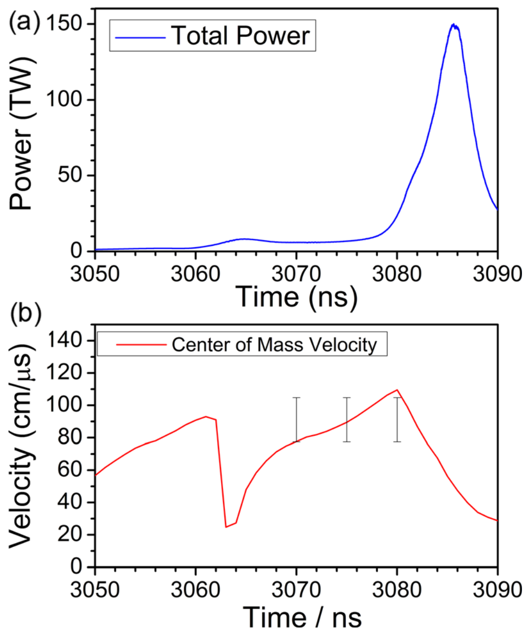

FIG. 3. (a) Total radiation pulses for an MHD simulation of a 70 mm wire array. (b) Center-of-mass velocity from the simulation, along with the average velocity inferred from analyzing the simulated radiation pulse by the same method used in Figure 2.

hence, when using the time delay between the two x-ray pulses to determine the characteristic velocity, the deceleration does not significantly impact the velocity measurement. Although we only have a limited dataset of Doppler splitting data from these experiments where this is seen, the velocities are significantly lower than the center of mass velocities seen in the simulation, consistent with Doppler measurements sampling the radiating plasma after kinetic energy has been thermalized. We note, however, that the time- and space-resolved natures of the previously reported Doppler measurements[10] are critical for understanding the detailed stagnation dynamics of large diameter z-pinches. Hence, the current technique, which is well suited for comparing multiple different shots, complements earlier work with Doppler measurements that are ideal for examining the detailed time evolution of the implosion.

IV. TREND WITH IMPLOSION VELOCITY

The radiation of K-shell photons from a wire array implosion is determined by a balance between competing effects. While a high velocity, symmetrical implosion leads to high electron temperatures, and efficient K-shell emission, high velocity implosions require rapid accelerations, and thus are more susceptible to the growth of magneto-Rayleigh-Taylor (MRT) instabilities. Hence, the highest K-shell yield will occur when the implosion velocity is sufficient to create high electron temperature ($\sim$5 keV), provided the acceleration is not so large that significant MRT disruption of the implosion occurs.

To study this balance, experiments were performed using three different initial wire array diameters (65 mm, 70 mm, and 75 mm), with at least three masses for each diameter. Nested wire arrays were used to minimize the growth of Magneto-Rayleigh-Taylor and other instabilities.[21] Each experiment used a nested wire array with an inner array mass and diameter that were half those of the outer array. By varying both the total mass and the outer array diameter, we have two separate controls on the implosion velocity. These different wire arrays were designed to have implosion velocities in the range of 70 to $\sim$130 cm/μs ($\eta \sim 1.4$–2.2).

The emitted K-shell and total powers from all of the shots are summarized in Figure 4. The different implosion

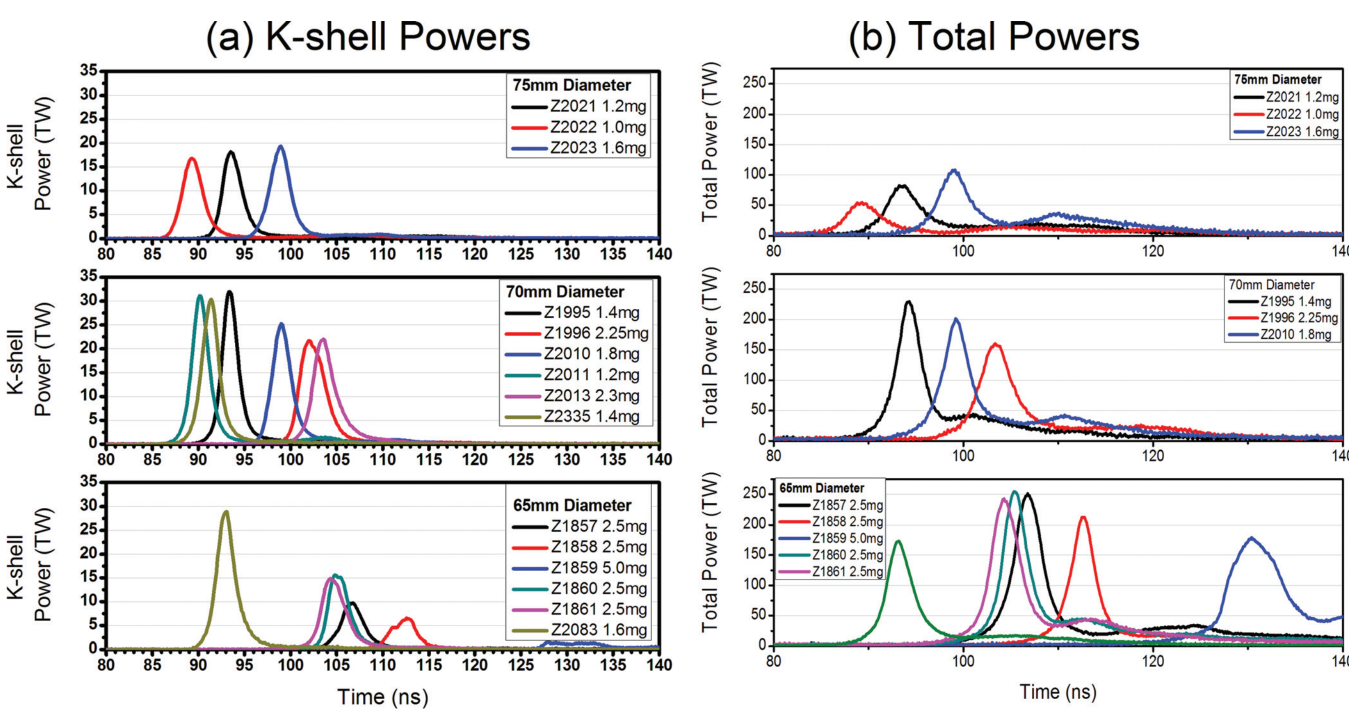

FIG. 4. Radiated K-shell and total power pulses for different array configurations. At each of three different initial diameters, multiple masses were fielded, leading to varying implosion times. On each plot, all different masses used at a given diameter are shown. Uncertainties in the K-shell powers are $\sim$15% and in total powers are $\sim$10%.

times at each diameter result from the different initial load masses.[2] Overall, the data indicate that implosion times of ∼93 ns provide the highest K-shell powers, with the 70 mm array at this implosion time providing the highest K-shell power of 32 TW.

Of the different experiments shown in Figure 4, the 75-mm-diameter experiments require the largest acceleration and reach the highest implosion velocities. Hence, these 75-mm-diameter experiments are most susceptible to the MRT instability. While not shown here, self-emission imaging indicates that these pinches have considerable disruption along the pinch axis and non-uniform emission, indicative of MRT instability. Evidence of MRT instability can also be seen directly in the radiated power pulses since, to first order, for a given radial width of an imploding plasma shell, the x-ray pulse will become narrower for a faster implosion. If MRT instability is present, this will broaden the x-ray pulse due to the spreading of material as it streams toward the axis. As seen in Figure 4, the 70 mm implosions show a narrower x-ray total and K-shell x-ray pulses than the 65 mm implosions for a given implosion time, while the 75 mm data show broader x-ray pulses. The decrease in pulsewidth from 65 mm to 70 mm is likely due to the higher implosion velocity expected for the larger diameter array. While the 75 mm arrays should have an even higher implosion velocity than the 70 mm loads (and therefore an even narrower pulse), the competing effects are no longer balanced and the effects of the MRT instability are more prevalent, broadening the pulse. The increased effect of MRT instability for the 75 mm experiments is also evident through the smoothing of the interaction pulse, making it indiscernible for two out of the three 75 mm experiments.

From Figure 4, we see that both the total and K-shell emission vary with the variations in diameter and mass. In Figure 4, the heavier arrays are able to radiate higher total yields (and generally higher total powers). Due to the longer implosion time of these arrays, the generator is able to do significantly more $\mathbf{J} \times \mathbf{B}$ work on them, leading to a higher coupled magnetic energy, even though the peak implosion velocity is slower. In fact, the 2.5 mg arrays shown in the lower panel of Figure 4(b) radiated ∼2.4 MJ total yield, with peak power of 260 TW, which is comparable to the peak power radiated by previous compact W wire arrays.[6,21] In contrast, the K-shell yield and power for this array is half that radiated by the lighter arrays. This result was expected given the much lower implosion velocities. The heavier arrays have more ions, so even though they have higher total coupled energy, the coupled energy per ion is lower than that of the lighter arrays. This can be directly observed in the data by comparing the variation of K-shell and total yields with the implosion velocities, as shown in Figure 5. Uncertainty in the calibration of the PCDs and bolometers, the need to extrapolate these from a limited view of the source to the full pinch height, and uncertainties in the spectral shape all lead to the uncertainties shown in the yields in Figure 5, and in the powers and yields shown in later plots. As the implosion velocity is increased, the imploded plasma becomes more efficient at radiating in the K-shell, while it becomes less efficient at radiating softer emission. These results are consistent with previous scaling theories, which have stated that the implosions that achieve velocities ∼110 cm/μs, and agree with previous data from Z prior to the refurbishment.[1] The peak K-shell power and yield for 1.4-mg, 70-mm wire arrays are a factor of 2 and 1.3 higher, respectively, than those obtained prior to the refurbishment of Z (Ref. 1) due to the higher current available to drive experiments on the refurbished version of the Z generator.

Time-integrated x-ray spectroscopy with a LiF crystal was used to determine plasma parameters attained during the stagnation phase of the implosion, via the calculations shown in Figure 1. Figure 6 shows time-integrated spectra collected during these experiments, normalized to the peak of the Fe He-α line. As shown in Figure 1, the ratio of the Fe He-α to the Fe Ly-α lines can provide a good diagnostic for the temperature of the pinch, so our discussion now centers on these lines. Figure 6 shows that there is considerable variation in the relative intensity of the Fe Ly-α line, ranging from 20% of the peak of the He-α line in the lighter 70 mm experiments to a few % in the heavier 65 mm arrays, corresponding to a significantly lower temperature in the smaller diameter heavy (i.e., slower) implosions compared to the lighter, larger diameter (i.e., faster) implosions.

Using the Fe He-α to Fe Ly-α line ratio, we can infer the temperature for each of the experiments shown in Figure 6;

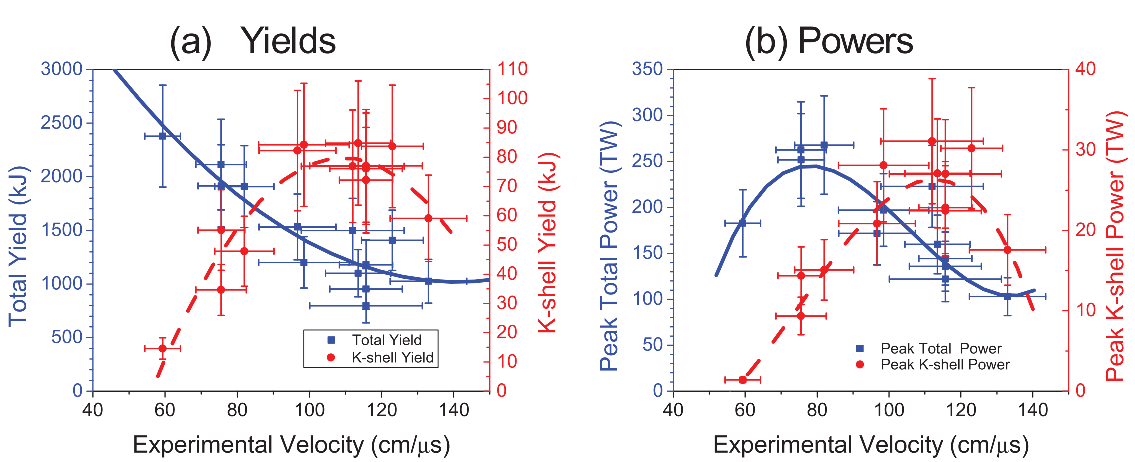

FIG. 5. Variation of the experimental total (blue) and K-shell yields (red) for different implosion velocities (inferred from experiments). Fits to the trend in each plot are shown.

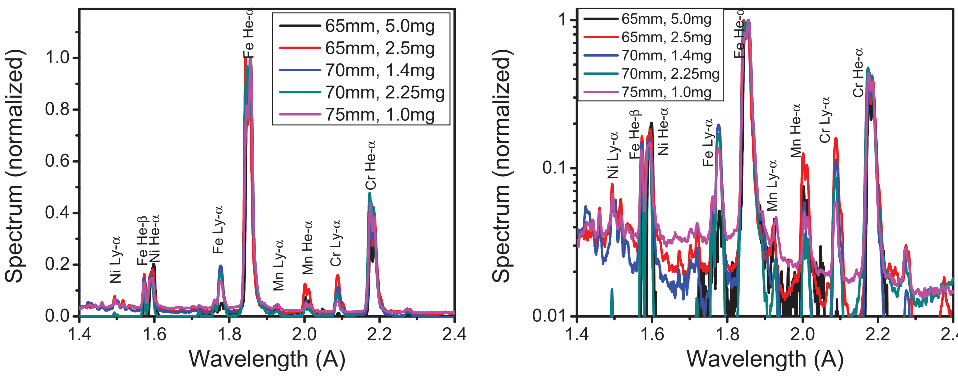

FIG. 6. Spectra for 5 different shots. The major emission lines are identified. The Fe Ly-α and He-α lines provide a temperature diagnostic. The data are shown on a linear scale (left) and logarithmic scale (right).

these results, plotted as a function of the measured implosion velocity, are shown in Figure 7(a). Uncertainties in these temperatures are based on uncertainties in the spectral shape and the limitations of the modeling shown in Figure 1. Given the temperatures for the different pinches, the radiated K-shell powers imply that the majority of the experiments reach Fe ion densities of $1.5 \times 10^{20}\,\mathrm{cm}^{-3}$; given that the stainless steel is only 75% Fe, this equates to total ion densities of $2.1 \times 10^{20}\,\mathrm{cm}^{-3}$.

In the plot in Figure 7(a), there is a direct correlation between the implosion velocity and the conditions reached in the pinch. The experiments with implosion velocities ~110 cm/μs reach stagnation temperatures near 5 keV, while the experiments with lower implosion velocities (~60 cm/μs) reach only ~3.5 keV.

At the fastest implosion velocities (>120 cm/μs), the K-shell yield and power are decreased. This could be the effect of the enhanced MRT instability for these faster implosion velocities or the decreased mass of these implosions. The analysis of the temperature of these stagnated columns helps to identify which of these effects is most likely to cause the drop in K-shell output.

The drop in temperature at high implosion velocity is consistent with a decrease in the performance of the 75-mm-diameter loads due to a larger effect of the MRT instability on the implosion: the pinch uniformity is insufficient to lead to good conversion of kinetic energy into thermal energy.

The effect that the variation in temperature has on the relative intensities of the K-shell and total yields is shown in Figure 7(b), which includes all three initial load diameters. There is a clear trend in the data, showing that the highest temperature pinches at ~5 keV are able to radiate ~5%–10% of the emission in the K-shell, whereas the colder pinches (~3.5 keV) only radiate ~1% of the emission in the K-shell. The best fit line to the fractional K-shell yield in Fig. 7(b) roughly follows exp(−Ek/Te), where Ek ~ 20 keV. The sum of all the Fe ionization potentials from neutral through Li-like is 16.5 keV. The 20 keV fit factor is indicative of the total ionization energy needed to get to the He-like ground state, plus a few keV extra needed for efficient excitation of the lines.

V. DISCUSSION

Experiments have studied high velocity (60–130 cm/μs) magnetically driven stainless steel wire array implosions. Experimentally determining the velocities of these implosions has allowed a detailed study of how this velocity affects both the plasma conditions in the stagnated pinch and the ability of the pinch to radiate in the K-shell and the total emission.

Low velocity implosions are very effective at radiating soft x-rays. The total radiated yield is highest (2.5 MJ) for the slowest velocity implosion (~60 cm/μs). The highest total x-ray power (250 TW) is radiated by ~80 cm/μs implosions.

For K-shell emission, the pinch must achieve higher electron temperatures. The data show that the plasma temperature is strongly dependent on the implosion velocity, with

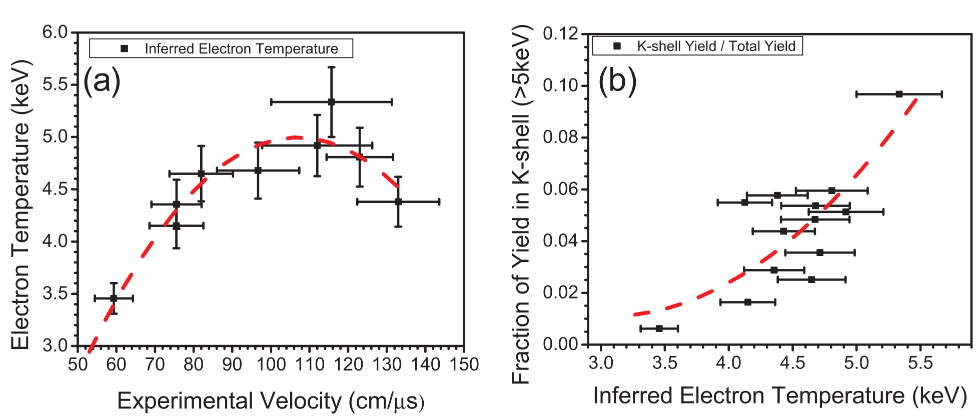

FIG. 7. (a) Variation of temperature with implosion velocity. (b) Fraction of total emission radiated in K-shell as a function of inferred temperature (from line ratios) for different masses at 65 mm, 70 mm, and 75 mm initial diameters. In (a), only those shots with a clean interaction pulse are shown. Fits to the trend in each plot are shown.

$\sim$110 cm/μs implosions reaching temperatures $\sim$5 keV, which is the highest temperature ever observed for stainless steel wire arrays. These high temperatures enable efficient radiation from K-shell transitions, with unprecedented radiated K-shell powers ($\sim$30 TW, a 2$\times$ improvement over previous stainless steel wire array experiments) and yield ($\sim$80 kJ, a 30% increase over previous experiments).

Experiments with the highest implosion velocities are unable to radiate efficiently because of the negative effect that magneto-Rayleigh-Taylor instabilities have on the pinch convergence, preventing the stagnated pinch from achieving high electron temperatures.

The higher currents on the refurbished Z generator allow the stagnated columns to achieve simultaneously high temperatures and high densities. Prior to the refurbishment there was considerably more variation in the densities obtained with different setups; however, in all of the present experiments, analysis indicates that densities $\sim 10^{20}\,\mathrm{cm}^{-3}$ were present, with the majority of the pinches 10%–20% smaller in diameter than in previous experiments. Stated differently, to radiate the 30 TW peak K-shell powers obtained in the present experiments requires high temperatures ($\sim$5 keV), densities ($\sim 10^{20}\,\mathrm{cm}^{-3}$), and ionization states ($Z \sim 24$), that can only be obtained if the coupled energy is sufficient to compress the final stagnated column to pressures $(Z+1)NkT \sim 40$ Mbar. Overall, the increase in coupled current from 17 MA to 20 MA due to the refurbishment of Z has enabled an increase in the temperatures and densities achieved in the stagnated pinch compared to previous data, allowing both an increase in the fraction of the total emission that is radiated in the K-shell and in the K-shell yield itself.

ACKNOWLEDGMENTS

The authors would like to thank all of the individuals who participated in these experiments at Z, including the Z Diagnostics group, the Z Center Section team, Load Hardware Designers, Hardware and Wire Array Assembly, Electrical Diagnostics and Z Operations.

Sandia National Laboratories is a multiprogram laboratory managed and operated by Sandia Corporation, a wholly owned subsidiary of Lockheed Martin Corporation, for the U.S. Department of Energy's National Nuclear Security Administration under Contract No. DE-AC04-94AL85000.

[1]C. A. Coverdale, C. Deeney, P. D. LePell, B. Jones, J. Davis, R. W. Clark, J. P. Apruzese, J. W. Thornhill, and K. G. Whitney, Phys. Plasmas **15**, 023107 (2008).
[2]D. D. Ryutov, M. S. Derzon, and M. K. Matzen, Rev. Mod. Phys. **72**, 167 (2000).
[3]K. G. Whitney, J. W. Thornhill, J. P. Apruzese, and J. Davis, J. Appl. Phys. **67**, 1725 (1990).
[4]J. W. Thornhill, K. G. Whitney, and J. Davis, J. Quant. Spectrosc. Radiat. Transf. **44**, 251 (1990).
[5]J. W. Thornhill, A. L. Velikovich, R. W. Clark, J. P. Apruzese, J. Davis, K. G. Whitney, P. L. Coleman, C. A. Coverdale, C. Deeney, B. Jones, and P. D. Lepell, IEEE Trans. Plasma Sci. **34**, 2377 (2006).
[6]M. E. Cuneo, R. A. Vesey, D. B. Sinars, J. P. Chittenden, E. M. Waisman, R. W. Lemke, S. V. Lebedev, D. E. Bliss, W. A. Stygar, J. L. Porter, D. G. Schroen, M. G. Mazarakis, G. A. Chandler, and T. A. Mehlhorn, Phys. Rev. Lett. **95**, 185001 (2005).
[7]D. J. Ampleford, C. A. Jennings, S. V. Lebedev, S. N. Bland, M. E. Cuneo, D. B. Sinars, S. C. Bott, G. N. Hall, F. Suzuki-Vidal, J. B. A. Palmer, and J. P. Chittenden, Phys. Plasmas **19**, 122711 (2012).
[8]M. E. Cuneo, D. B. Sinars, E. M. Waisman, D. E. Bliss, W. A. Stygar, R. A. Vesey, R. W. Lemke, I. C. Smith, P. K. Rambo, J. L. Porter, G. A. Chandler, T. J. Nash, M. G. Mazarakis, R. G. Adams, E. P. Yu, K. W. Struve, T. A. Mehlhorn, S. V. Lebedev, J. P. Chittenden, and C. A. Jennings, Phys. Plasmas **13**, 056318 (2006).
[9]C. A. Jennings, M. E. Cuneo, E. M. Waisman, D. B. Sinars, D. J. Ampleford, G. R. Bennett, W. A. Stygar, and J. P. Chittenden, Phys. Plasmas **17**, 092703 (2010).
[10]B. Jones, C. A. Coverdale, C. Deeney, D. B. Sinars, E. M. Waisman, M. E. Cuneo, D. J. Ampleford, P. David LePell, K. R. Cochrane, J. Ward Thornhill, J. P. Apruzese, A. Dasgupta, K. G. Whitney, R. W. Clark, and J. P. Chittenden, Phys. Plasmas **15**, 122703 (2008).
[11]J. P. Apruzese, K. G. Whitney, J. Davis, and P. C. Kepple, J. Quant. Spectrosc. Radiat. Transf. **57**, 41 (1997).
[12]J. P. Apruzese, J. Quant. Spectrosc. Radiat. Transf. **34**, 447 (1985).
[13]J. P. Apruzese, J. W. Thornhill, K. G. Whitney, J. Davis, C. Deeney, and C. A. Coverdale, Phys. Plasmas **8**, 3799 (2001).
[14]K. G. Whitney, J. W. Thornhill, J. L. Giuliani, Jr., J. Davis, L. A. Miles, E. E. Nolting, V. L. Kenyon, W. A. Speicer, J. A. Draper, C. R. Parsons, P. Dang, R. B. Spielman, T. J. Nash, J. S. McGurn, L. E. Ruggles, C. Deeney, R. R. Prasad, and L. Warren, Phys. Rev. E **50**, 2166–2174 (1994).
[15]B. Jones, C. A. Jennings, J. E. Bailey, G. A. Rochau, Y. Maron, C. A. Coverdale, E. P. Yu, S. B. Hansen, D. J. Ampleford, P. W. Lake, G. Dunham, M. E. Cuneo, C. Deeney, D. V. Fisher, V. I. Fisher, V. Bernshtam, A. Starobinets, and L. Weingarten, Phys. Rev. E **84**, 056408 (2011).
[16]R. B. Spielman, Rev. Sci. Instrum. **66**, 867 (1995).
[17]H. C. Ives, W. A. Stygar, D. L. Fehl, L. E. Ramirez, S. C. Dropinski, D. L. Wall, J. S. Anctil, J. S. McGurn, J. H. Pyle, D. L. Hanson, B. N. Allison, M. J. Berninger, E. A. Bryce, G. A. Chandler, M. E. Cuneo, A. J. Fox, T. L. Gilliland, C. L. Haslett, R. J. Leeper, D. F. Lewis, M. A. Lucero, M. G. Mazarakis, D. H. McDaniel, J. L. McKenney, J. A. Mills, L. P. Mix, J. L. Porter, M. B. Ritchey, L. E. Ruggles, J. F. Seamen, W. W. Simpson, R. B. Spielman, J. A. Torres, M. F. Vargas, T. C. Wagoner, L. K. Warne, and M. W. York, Phys. Rev. ST Accel. Beams **9**, 110401 (2006).
[18]T. J. Nash, M. S. Derzon, G. A. Chandler, D. L. Fehl, R. J. Leeper, J. L. Porter, R. B. Spielman, C. Ruiz, G. Cooper, J. McGurn, M. Hurst, D. Jobe, J. Torres, J. Seaman, K. Struve, S. Lazier, T. Gilliland, L. A. Ruggles, W. A. Simpson, R. Adams, J. A. Seaman, D. Wenger, D. Nielsen, P. Riley, R. French, B. Stygar, T. Wagoner, T. W. L. Sanford, R. Mock, J. Asay, C. Hall, M. Knudson, J. Armijo, J. McKenney, R. Hawn, D. Schroen-Carey, D. Hebron, T. Cutler, S. Dropinski, C. Deeney, P. D. LePell, C. A. Coverdale, M. Douglas, M. Cuneo, D. Hanson, J. E. Bailey, P. Lake, A. Carlson, C. Wakefield, J. Mills, J. Slopek, T. Dinwoodie, and G. Idzorek, Rev. Sci. Instrum. **72**, 1167 (2001), and references therein.
[19]T. W. L. Sanford, M. E. Cuneo, D. E. Bliss, C. A. Jennings, R. C. Mock, T. J. Nash, W. A. Stygar, E. M. Waisman, J. P. Chittenden, M. G. Haines, and D. L. Peterson, Phys. Plasmas **14**, 052703 (2007).
[20]J. P. Chittenden, S. V. Lebedev, S. N. Bland, F. N. Beg, and M. G. Haines, Phys. Plasmas **8**, 2305 (2001).
[21]C. Deeney, M. R. Douglas, R. B. Spielman, T. J. Nash, D. L. Peterson, P. L'Eplattenier, G. A. Chandler, J. F. Seamen, and K. W. Struve, Phys. Rev. Lett. **81**, 4883 (1998).